The Effect of Temperature and Solution pH on the Nucleation of Tetragonal Lysozyme Crystals

Russell A. Judge,* Randolph S. Jacobs,# Tyralynn Frazier,§ Edward H. Snell,¶ and Marc L. Pusey¶

*Alliance for Microgravity Material Science and Applications, NASA/Marshall Space Flight Center, Huntsville, Alabama 35812;
#Department of Chemical Engineering, University of Alabama in Huntsville, Huntsville, Alabama 35899; §Biochemistry Department, Michigan State University, East Lansing, Michigan 48825; and ¶Biophysics SD48, NASA/Marshall Space Flight Center, Huntsville, Alabama 35812 USA

ABSTRACT   Part of the challenge of macromolecular crystal growth for structure determination is obtaining crystals with a volume suitable for x-ray analysis. In this respect an understanding of the effect of solution conditions on macromolecule nucleation rates is advantageous. This study investigated the effects of supersaturation, temperature, and pH on the nucleation rate of tetragonal lysozyme crystals. Batch crystallization plates were prepared at given solution concentrations and incubated at set temperatures over 1 week. The number of crystals per well with their size and axial ratios were recorded and correlated with solution conditions. Crystal numbers were found to increase with increasing supersaturation and temperature. The most significant variable, however, was pH; crystal numbers changed by two orders of magnitude over the pH range 4.0–5.2. Crystal size also varied with solution conditions, with the largest crystals obtained at pH 5.2. Having optimized the crystallization conditions, we prepared a batch of crystals under the same initial conditions, and 50 of these crystals were analyzed by x-ray diffraction techniques. The results indicate that even under the same crystallization conditions, a marked variation in crystal properties exists.

INTRODUCTION

Nucleation and crystal growth kinetics in connection with the amount of material available for crystal growth determine the number and volume of the crystals produced. In the pursuit of a small number of crystals with a suitable volume (i.e., 0.1–0.4 mm in each dimension) for x-ray structure analysis, an understanding of nucleation rates is advantageous. From classical nucleation theory the variables that effect the nucleation rate are the supersaturation, temperature, and interfacial tension. Increases in temperature or supersaturation, or a decrease in the interfacial tension are expected to produce an increased nucleation rate (Mullin, 1993).

Whereas many nucleation studies have been performed for small molecules, nucleation studies for biological macromolecules are limited. Some studies have focused on determining nucleation parameters. Light scattering has been used to examine molecular interactions leading to nucleation (Kam et al., 1978; Pusey, 1991) and to estimate the interfacial tension and the size of the critical nucleus (Mikol et al., 1989; Malkin and McPherson, 1993). Other investigators have used batch crystallization and followed the drop in bulk solution concentration (or the increase in crystal content) over time, combining nucleation and growth kinetics to determine nucleation parameters (Ataka and Asai, 1990; Elgersma et al., 1992; Pusey, 1992; Bessho et al., 1994; Vekilov et al., 1996). Apart from the work of

Malkin and McPherson (1993), all of these investigators have used lysozyme as their model protein. Stirred vessels have also been used to measure ovalbumin (Judge et al., 1995) and thermolysin (Harano et al., 1989) nucleation thresholds and the width of the metastable zone.

Few studies, however, have focused on measuring the effect of solution conditions on nucleation rates by specifically counting and sizing crystals. Ries-Kautt and Ducruix (1992) made the general observation that lysozyme crystals appeared faster and in larger numbers with increasing supersaturation. Alderton and Fevold (1946) reported that in initial lysozyme concentrations of 40 mg/ml, in 5% NaCl solutions, crystallization was copious at pH 3.5, moderate at pH 4.8, and very slight at pH 5.8, indicating a strong effect of pH. Elgersma et al. (1992) (their figure 4) also report an effect of pH on lysozyme crystal numbers, as large numbers of crystals can be seen at pH 4.0 ($\ln(c/s) = 1.2$), whereas fewer crystals are present at pH 6.0 ($\ln(c/s) = 1.6$). Both experiments were conducted at 5°C with 3% NaCl. In batch lysozyme crystallization at low supersaturation, Ataka and Tanaka (1986) found no clear trend in crystal numbers with increases in supersaturation or salt concentration. Crystal size was found over the pH range 4.2–5.5 to reach a maximum at pH 4.6. Crystal size was also found to be at maximum at a supersaturation ratio of 3. The effect of supersaturation on the number of thermolysin crystals was reported by Sazaki et al. (1994), who observed that the number of crystals initially decreases and then increases with increasing supersaturation. This is thought to be due to the postulated growth mechanism of thermolysin. Monomers are believed to form aggregates (reversibly self-associating clusters) of constant size, and it is these aggregates that then form the crystal. They indicate that this may also

be what is happening in the lysozyme study of Ataka and Tanaka (1986). Sazaki et al. (1994) also comment that the final number of crystals may not equal the number of initial nuclei if aggregates are the growth unit of the macromolecule.

To further examine nucleation behavior, this study investigates the effects of solution conditions (initial supersaturation, temperature, and solution pH) on chicken egg white lysozyme nucleation rates and crystal sizes. Having thus determined solution conditions at which well-formed crystals of suitable volume could be reproducibly obtained, an x-ray analysis of 50 crystals was undertaken to examine the extent of variation in crystal parameters. The results indicate the magnitude of the effect of differing solution conditions on crystal numbers and highlight an interesting variation in crystal properties for crystals produced under optimal crystallization conditions.

MATERIALS AND METHODS

Fresh chicken eggs were obtained from a local egg farm run by Mr. Ernest Joe Adair (Woodville, AL), with permission from Hudson Foods, National Egg Products Company (Social Circle, GA). Lysozyme was extracted directly from the fresh chicken egg white, using an adaptation of the chromatography method of Rhodes et al. (1958) given elsewhere (Judge et al., 1998). The lysozyme was extensively dialyzed against 0.1 M sodium acetate buffer at the pH set for each experiment, concentrated using Amicon ultrafiltration units with YM3 membranes (Amicon, Beverly, MA), and stored at 4°C. Lysozyme concentrations were calculated based on A(1%, 1 cm, 281.5 nm) = 26.4 (Aune and Tanford, 1969). Protein purity was determined by SDS-PAGE (sodium dodecyl sulfate-polyacrylamide gel electrophoresis) analysis with enhanced silver staining, using a Phastsystem with Phastgel gradient 8–25% gels (Pharmacia LKB Biotechnology, Piscataway, NJ). Sodium acetate buffer was made by titration of 0.1 M acetic acid solution with sodium hydroxide until the desired pH was obtained. All experiments were conducted at 5% (w/v) NaCl concentration. Crystallization buffers were passed through a 0.02-μm filter before use. Lysozyme stock solution was centrifuged at 6000 × g for 10 min (Eppendorf centrifuge 5413; Brinkmann Instruments, Westbury, NY) directly before use to avoid the effects of solution aging on crystal numbers thought to be caused by fungi particles (Chayen et al., 1993).

The batch nucleation experiments were conducted using 96 well Cooke Microtiter polystyrene plates (Dynatech Laboratories, Alexandria, VA). The wells are U-shaped, with a 7-mm diameter and a capacity of ~250 μl. The batch method allows an exact initial supersaturation value to be obtained and used to compare nucleation results, whereas in the vapor diffusion or dialysis method the supersaturation at which crystals are formed is unknown. The plates were thoroughly rinsed with distilled water to remove dust particles and allowed to dry in an inverted position. During filling, the plates were set on a damp paper towel to prevent static electricity build-up. Lysozyme solutions of different initial concentrations were prepared by manually combining protein in 0.1 M sodium acetate buffer with an equal volume of 0.1 M sodium acetate buffer containing 10% NaCl, at the same pH, in an 1.5 ml Eppendorf tube (Daigger and Company, Wheeling, IL). The solution was mixed by gently inverting the tube twice and then quickly dispensed in 50-μl aliquots to a row of 10 wells on the plate. For all of the experiments conducted in this study, a fixed solution volume of 50 μl per well was used. As nucleation is expected to be a stochastic process, for each plate 10 wells per sample were used to provide a broader sample of results. Lower concentration lysozyme solutions were made and dispensed to the plate first, with the highest concentration solution made and dispensed last. In all, six lysozyme concentrations covering a range of supersaturation were dispensed on each plate. The plate was sealed with clear tape and placed in an incubator. The

protein concentration in each of the Eppendorf tubes from which solution was dispensed to the plate was measured by UV absorbance immediately after the plate was completed. Plates were prepared individually in duplicate and, occasionally, triplicate. Incubator temperatures were set at 4, 10, 15, and 18°C. To ensure that only tetragonal crystals were formed, 18°C was the highest temperature used, so as to stay well below the tetragonal/orthorhombic phase transition, which is reported to occur at ~25°C (Jolles and Berthou, 1972). The pH values investigated were 4.0, 4.6, 4.8, and 5.2. The plates were analyzed after 1 week.

To test for water loss from the crystallization plates, a plate containing only lysozyme samples (33.7, 16.8, 8.5 and 4.3 mg/ml) in 0.1 M sodium acetate buffer, pH 4.0, was prepared in the same manner as given above. Two wells for each sample solution were filled with 50 μl each, and the plate was incubated at 18°C. After 1 week the changes observed in the lysozyme concentrations were less than 2%. The effect of water loss on the crystallization over the course of the experiments was therefore considered negligible.

A low-magnification microscope with an attached CCD video camera was used in combination with a computer containing a frame grabber board to record images of each well. At a later time Image Pro Plus software (Southern Micro Instruments, Atlanta, GA) was used to enlarge and display the images and to manually tag and count crystals. For wells containing small numbers of crystals, all of the crystals in the well were counted. Where wells contained large numbers of crystals (~1000), the image was divided into halves or quarters. That portion of the image was further enlarged, and the crystals were manually counted. The total for the well then was two times the count for halves or four times the count for quarters. This technique is based on the assumption that the crystals are uniformly distributed in the well. The consistently good agreement in crystal numbers found for each group of 10 wells at the same crystallization conditions indicates the applicability of the technique.

Crystal size and axial ratios were measured using a Zeiss Axioplan microscope (Carl Zeiss, Thornwood, NY) connected to an Argus-10 image processor (Hamamatsu Photonics K. K., Hamamatsu City, Japan), which had been calibrated with a standard size grid. In this case a higher magnification could be used, focusing on only a small portion of the well at a time, so that individual crystals could be more easily viewed and measured. Five crystals per well were randomly selected, and the distance between parallel {110} faces and the distance between the apexes of the {101} faces were measured using crystals suitably aligned with the optical axis. As only five crystals per well were sized (giving 50 per initial concentration per plate), these measurements constitute an estimate of the crystal size and dimensions. This technique, however, provided sufficient detail to quantify the effect of the crystallization variables studied in this work.

The depth of the nucleation plates impeded careful mounting of the crystals for x-ray analysis. For this reason, pseudo-batch crystallization was conducted with sitting drop plates. This was done by placing 50 μl of crystallization solution in the inside well and adding 1.4 ml of the same solution without protein to the outside well of the sitting drop plate. The crystallization conditions for the x-ray diffraction analysis were chosen as a result of the findings in the nucleation rate work. This choice was a trade-off between ensuring a constant illuminated volume (with a small crystal completely illuminated in the x-ray beam) and the data collection time from diffracting volume considerations. In the end, based on the results described later, 120 pseudo-minibatch crystallization wells were prepared with 0.1 M sodium acetate buffer (pH 5.2), 5% NaCl, and 19.7 mg/ml initial lysozyme concentration. These plates were prepared at the same time and stored in the same incubator at 18°C. Under these conditions the lysozyme solubility is 2.13 mg/ml (Cacioppo and Pusey, 1991), giving an initial supersaturation $\ln(c/s)$ of 2.2. Fifty crystals from these plates were used for x-ray analysis. Crystals were mounted in 0.7-mm-diameter glass capillaries by standard methods (King, 1954; Holmes and Blow, 1966), leaving some mother liquor in the capillary to maintain the crystal in a humid atmosphere. The crystal mounting was performed by the same person throughout, with samples mounted individually before each x-ray data collection. The epoxy resin used for sealing the capillary has a slight heating effect on setting. This is negligible for the small amount of resin used and is less than that experienced when wax is used. Every effort was

made to ensure the crystals were mounted such that the same volume would be illuminated during the x-ray data collection, although the crystals were not specifically oriented. The crystals proved to be slightly anisotropic in depth and width, so they were positioned such that the maximum width or depth was parallel to the beam before data collection was started. The average dimensions were $0.51 \times 0.34 \times 0.25$ mm ($\pm$ 7, 6, 8%, respectively). The anisotropy results from crystals settling and growing on the bottom of the well, where the face in contact with the well wall is restricted from further growth. Identical data collection parameters were used ($80°$ of data in 40, $2°$ oscillations of 10 min exposure). An Raxis IIC image plate was used as the detector, with CuKα x-rays provided by a Rigaku RU200 rotating anode at 40 mA and 70 kV, with a 0.3-mm pinhole collimator and graphite monochromator. The crystal-to-detector distance was 96 mm, with data collection carried out at room temperature, $22 \pm 2°C$. Data were integrated using Denzo and reduced with Scalepack (Otwinowski and Minor, 1997) for comparison. In each case the crystal volume was measured.

RESULTS

Commercial lysozyme preparations commonly contain a number of higher molecular mass protein impurities, including conalbumin (78 kDa), ovalbumin (45 kDa), and a lysozyme dimer (28 kDa) (Back, 1984; Thomas et al., 1996). Whereas impurities such as ovalbumin, conalbumin, and avidin appear to be excluded during lysozyme crystallization (Judge et al., 1998), the lysozyme dimer is incorporated (Skouri et al., 1995; Thomas et al., 1996). Lysozyme used in this study was checked by SDS-PAGE analysis with highly overloaded samples (10,000 ng per lane) to determine if such impurities were present. With enhanced silver staining no other protein bands could be identified (Fig. 1). This represents purity greater than 99.99% with respect to other protein species.
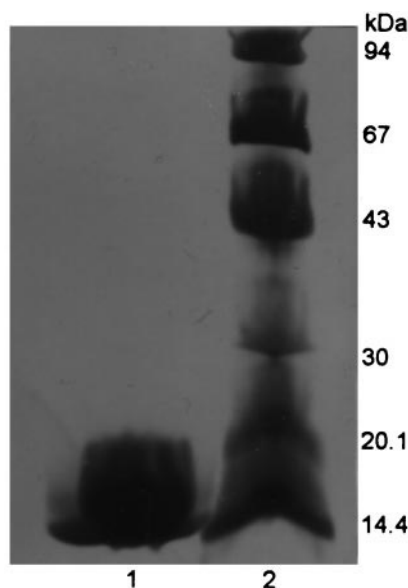
The reproducibility of the batch method for crystal numbers as a function of initial supersaturation is illustrated in Fig. 2 for the crystallization conditions at pH 4.8, 4°C. In this figure each symbol represents the average of 10 wells at the same initial supersaturation. The error bars represent 95% confidence limits based on the scatter of the data. The different symbols represent results from three separately prepared plates. In this study supersaturation is expressed as $\ln(c/s)$, where c is the bulk initial solution concentration and s is the solubility concentration. At these crystallization conditions no crystals were observed within the 1-week period at the lowest supersaturation value of $\sim$1.4. When we fit a simple straight line to the nonzero data, the intercept with the supersaturation axis gives an estimate of the metastable zone, which in terms of supersaturation is 1.85. Under these experimental conditions no crystals would be expected to form below this supersaturation within the 7-day period of crystallization. Throughout the study the metastable zone width was found to vary little with temperature. The solution pH, however, appears to have an effect, as at the lower pH values the average width of the metastable zone in terms of the supersaturation is 1.5, whereas at the higher pH values it is 1.9. It should be noted, however, that the width of the metastable zone is time dependent, and for longer duration experiments crystals are expected to appear at lower supersaturations (Mullin, 1993).

The results for the effect of temperature on the number of crystals produced per well at pH 4.0, 4.6, 4.8, and 5.2 are given in Fig. 3. In this figure each symbol represents an average of 20–30 data points. The crystal numbers in all cases increase linearly with supersaturation. The coefficients and fit to the data for all of the results are listed in Table 1. At a constant value of supersaturation, crystallization at higher temperatures was found to produce more crystals. This trend was observed at all of pH values used. In fact, crystal numbers not only increase with temperature but also appear to increase in proportion to increases in temperature. For example (for any specific pH, for values of
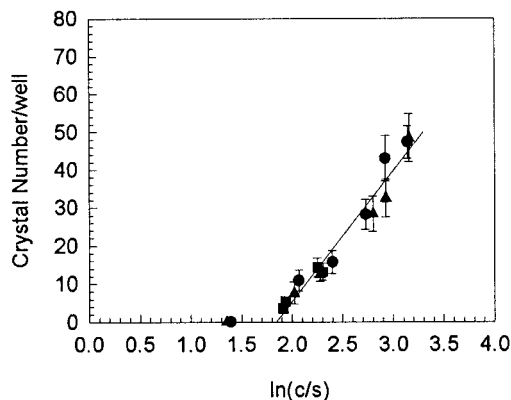

FIGURE 1 Lysozyme purity. SDS-PAGE gel with enhanced silver staining and high sample loading (10,000 ng). *Lane 1*: Lysozyme. *Lane 2*: Molecular weight markers. Note: No higher molecular weight impurity proteins are visible.

FIGURE 2 . Effect of supersaturation on crystal number at pH 4.8 and 4°C. Each symbol represents the average of 10 wells. The error bars represent 95% confidence limits based upon the variation of the data. The different symbols represent results from three separately prepared plates.
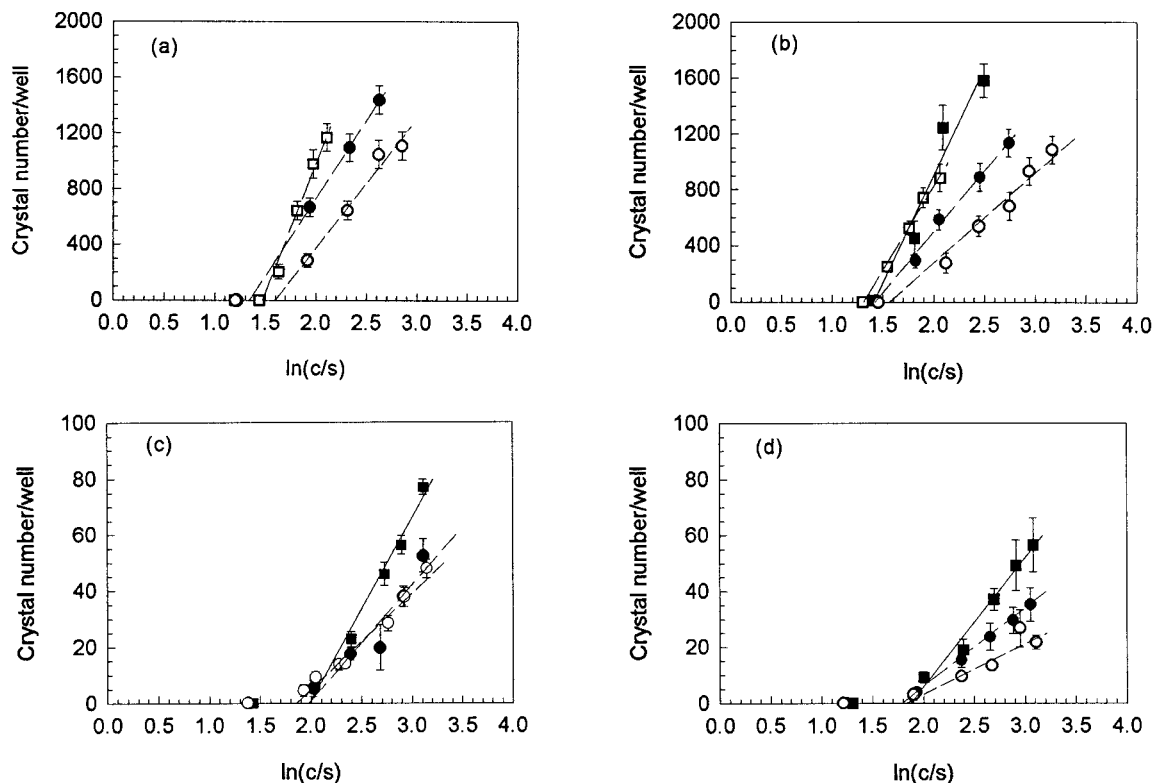
FIGURE 3　The effect of temperature on the number of crystals produced per well at (*a*) pH 4.0, (*b*) pH 4.6, (*c*) pH 4.8, and (*d*) pH 5.2. ■, 18°C; □, 15°C; ●, 10°C; ○, 4°C.

supersaturation at which crystals were produced at each temperature), the number of crystals at 18°C is approximately a factor of 1.7 times the number at 10°C, and the crystal number at 10°C is approximately a factor of 1.5 times the number at 4°C. The exception to this observation was pH 4.8, where the data at 10°C and 4°C are very close.

The solution pH also has a notable effect upon the number of crystals produced. This is summarized in Fig. 4, which presents data at each of the measured pH values at 4°C. The highest crystal numbers occur at pH 4.0. Taking a constant value of supersaturation, as the pH increases to pH 4.6 the crystal number drops by a factor of ~1.5, whereas the change of pH from 4.6 to 4.8 results in a drop by a factor of ~20. This is a significant change over a very narrow pH range. The change in crystal number between pH 4.8 and 5.2, barely noticeable because of the axis scale, is a factor of ~2. Similar changes in crystal number with pH were also obtained at 10°C.

The effect of pH on crystal size, defined in terms of the distance between parallel {110} faces, is illustrated in Fig. 5. Crystal size increases substantially with increases in pH

TABLE 1 Equation parameters for equations of the form $y = a + bx$ fit to the nucleation data, where y is the final number of crystals per well and x is the supersaturation, $\ln(c/s)$

pH	T (°C)	A	B	r^2	s (mg/ml)
4.0	15	−2722	1852	0.99	0.92
4.0	10	−1500	1116	0.99	0.54
4.0	4	−1476	926	0.97	0.28
4.6	18	−2147	1525	0.95	1.53
4.6	15	−1568	1198	0.99	1.18
4.6	10	−1235	867	0.99	0.82
4.6	4	−1004	642	0.97	0.47
4.8	18	−129	65	0.98	1.39
4.8	10	−81	41	0.91	0.68
4.8	4	−63	34	0.98	0.47
5.2	18	−86	46	0.98	2.13
5.2	10	−50	28	0.99	1.09
5.2	4	−33	18	0.87	0.83

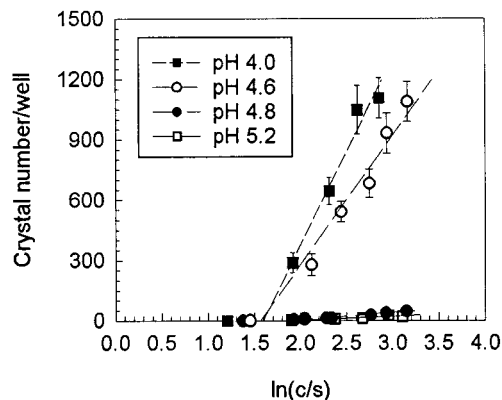Values of lysozyme solubility were taken from Cacioppo and Pusey (1991).

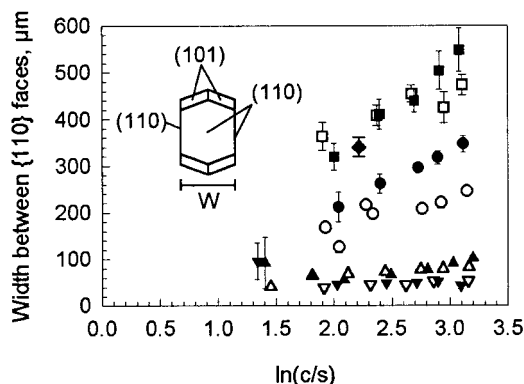FIGURE 4　The effect of solution pH on crystal number per well at 4°C.

FIGURE 5   The effect of pH and temperature on final crystal size (W), defined as the distance between parallel {110} faces. Symbols: at pH 5.2, 18°C (■) and 4°C (□); at pH 4.8, 18°C (●) and 4°C (○); at pH 4.6, 18°C (▲) and 4°C (△); at pH 4.0, 18°C (▼) and 4°C (▽). ◆, The pseudo-batch crystal size at pH 5.2, 18°C, $\ln(c/s) = 2.2$.
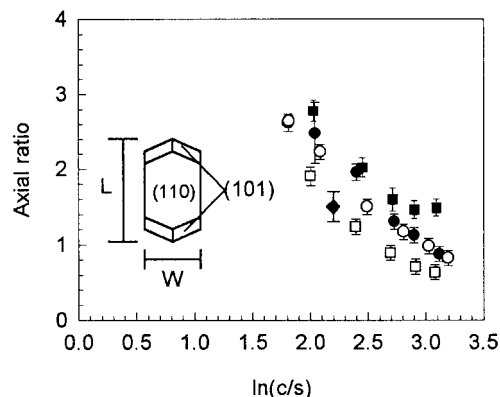

FIGURE 6   The effect of pH on the crystal axial ratio at 18°C. The axial ratio is defined as the distance between the apexes of the {101} faces (L) over the distance between parallel {110} faces (W). Symbols: □, pH 5.2; ●, pH 4.8; ○, pH 4.6; ■, pH 4.0; ◆, the pseudo-batch crystal result.

from 4.0 to 5.2, with the largest crystals ($\sim$320–550 μm) obtained at pH 5.2. Supersaturation appears to have a greater effect on crystal size at the higher pH values (pH 4.8 and 5.2). Here size appears to increase with supersaturation, whereas this trend is suppressed at the lower pH values (pH 4.0 and 4.6). This figure also gives an indication of the effect of temperature, showing final crystal sizes at 18°C and 4°C. Data at 10°C were not included, to preserve the clarity of the figure. No clear trend with temperature was observed at any pH value. For pH 4.8 and 4°C, four individual wells were chosen (two wells on each of two separate plates), and the size of every crystal in the well was measured. The details of this analysis are included in Table 2. The average variation from the mean size (based on 95% confidence limits) was found to be ±8%.

The effect of solution conditions on the axial ratio is illustrated in Fig. 6. For all of the batch crystallizations performed in this study, the axial ratio increases as the supersaturation decreases. This reflects the finding of Durbin and Feher (1986), who report that the growth rates of the {110} and {101} faces have a different concentration dependence, resulting in an elongation of the crystal at lower lysozyme concentrations. Although it is difficult to

identify a trend between the pH values 4.6 and 4.8, when we look at the values at pH 4.0 and 5.2 for the same supersaturation there appears to be a trend of decreasing axial ratios with increasing pH. No clear trend was found for the axial ratio with temperature, the variation in the data with temperature being negligible in comparison to the effect of pH (data not shown). Of the crystallization parameters, supersaturation, temperature, and pH, it is pH that has the strongest effect on crystal number and size. For the axial ratio both pH and supersaturation exhibit strong influences.

As the largest crystals with the lower axial ratios were obtained at pH 5.2, this pH was chosen for crystal growth in the pseudo-batch plates for x-ray analysis. With crystallization conditions of 18°C and an initial supersaturation of $\ln(c/s) = 2.2$, the pseudo-batch plates produced 15 ± 2 crystals/well. The average size was 340 μm ± 6% between parallel {110} faces and 510 μm ± 7% between the apexes of the {101} faces, giving an axial ratio of 1.5 ± 0.2. Using the equation parameters given in Table 1, 15 crystals/well is the number of crystals expected for a batch plate crystallization at these solution conditions. The average size between parallel {110} faces and the average axial ratios of crystals from the pseudo-batch plates have also been plotted in Figs. 5 and 6, respectively, for comparison. Given the comparison of crystal number, size, and axial ratio, the results from these two methods do appear to be in good agreement.

The pseudo-batch crystals grew in the tetragonal $P4_32_12$ space group with cell parameters $a = b \neq c$ and $\alpha = \beta = \gamma = 90°$. An average of 97.8% of the available data (6292 unique reflections) to 2.2 Å resolution was used for determining the cell parameters. Fig. 7 illustrates the variation in unit cell parameter c for the 50 crystals observed (one not diffracting). The data covers a range from 37.41 to 38.26 Å, with 50% of the data falling within the limits of the modal range of 38.0–38.1 Å. The average error for the determination of the c parameter was ±0.04 Å. The modal range is well within the range of values 37.89–38.50 Å, commonly

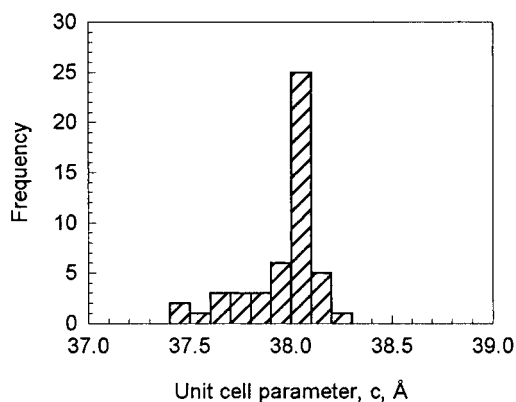**TABLE 2   Crystallization conditions, crystal number, mean size, and 95% confidence limits for four crystallization wells at pH 4.8, 5% NaCl**

	Crystallization well			
	A	B	C	D
T (°C)	10	10	4	4
$\ln(c/s)$	3.1	2.7	2.4	2.7
Crystal number	54	16	13	36
Mean size (μm)	253	269	236	216
95% confidence limit, ± μm	13	27	25	13

The wells were chosen randomly and have been designated A, B, C, or D as a convenient label. Note: Size is defined as the distance between parallel {110} faces.

FIGURE 7 Variation in the lysozyme $P4_32_12$ "c" unit cell parameter in a sample of 50 crystals grown from solutions prepared with the same initial conditions.

reported for tetragonal lysoyzme (Forsythe et al., 1997). A similar distribution is seen for the *a* cell parameter and other crystallographic "metrics." Fig. 8 illustrates the effect of time on the unit cell parameters. An area of concern had been the effect of aging on the samples, with each data set being collected sequentially. As can be seen, for this protein system, there seems to be no time dependence of the experiment. There was no correlation between the sequence of the data collection and any other crystallographic parameters that were measured.

DISCUSSION

In classical nucleation theory the number of crystals produced is expressed as a rate, i.e., the number of crystals produced per unit volume per unit time. In our experiments we have measured the number of crystals produced in a set volume over a single extended period. This makes the direct application of classical nucleation theory impractical. Nucleation theory, however, indicates that three variables, supersaturation, temperature, and interfacial tension, govern
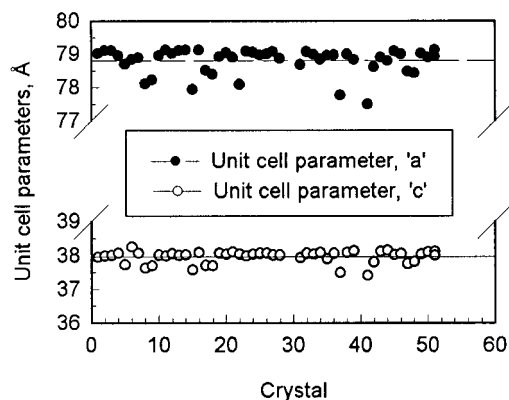

FIGURE 8 The lysozyme $P4_32_12$ "a" and "c" unit cell parameters for the 50 crystal sample plotted sequentially over the time of the experiments. The horizontal lines indicate average unit cell parameter values.

the process (Mullin, 1993). This applies whether the process is homogeneous or heterogeneous. In heterogeneous nucleation the interfacial tension is reduced as molecules interact with particles in solution or with vessel walls. Depending on the degree of interaction, changes in the interfacial tension may still have an effect on nucleation rates (Mullin, 1993; Boistelle and Astier, 1988). As these three variables drive the nucleation process, the changes in crystal numbers that are observed with varying solution conditions may reflect changes in the nucleation process that can be compared in general terms to that predicted by nucleation theory. In this respect, as indicated by Mullin (1993) and Boistelle and Astier (1988), crystal numbers are expected to increase with increases in supersaturation. The results of this study are in accordance with this prediction and with the findings of Ries-Kautt and Ducruix (1992), who also observed that lysozyme crystals appeared in larger numbers with increasing supersaturation. Interestingly, Ataka and Tanaka (1986), who also crystallized lysozyme in batch but at lower supersaturations ($\sim \ln(c/s)$ of 0.5–1.8) and over a much longer time (43 days or greater), reported that an increase in supersaturation did not necessarily result in an increased number of crystals. Duplicate runs confirmed their results. These experimental conditions are generally outside the scope of this present study and may point to other phenomena at low supersaturations over extended time.

At constant supersaturation an increase in crystal numbers with increasing temperature is another trend predicted by nucleation theory (Mullin, 1993; Boistelle and Astier, 1988). Again our results are in good agreement with this prediction. This points to the use of temperature as a tool for fine-tuning of protein crystal nucleation rates. The number of crystals produced at a given pH and chosen supersaturation could be increased or decreased by crystallizing at a higher or lower temperature. The findings of this study indicate that at a constant supersaturation a change of 10°C results in a change of lysozyme crystal numbers by a factor of ~ 2.3.

Our results also show a substantial effect of pH on crystal numbers with a change of two orders of magnitude over the pH range 4.0–5.2. Alderton and Fevold (1946), with initial lysozyme concentrations of 40 mg/ml in unbuffered 5% NaCl solutions, may be referring to this when they describe the crystallization to be copious at pH 3.5, moderate at pH 4.8, and very slight at pH 5.8. This effect of pH on crystal numbers appears to be independent of solution pH history. In this study protein solutions at pH 4.0 produce large numbers of crystals. When protein solution initially at pH 4.0 was dialyzed into buffer at pH > 4.6 and used in nucleation experiments at these pH values, small numbers of crystals were produced; increases in crystal number were observed when solutions initially at pH > 4.6 were changed to values closer to pH 4.0. Experiments were generally conducted around pH 4.0, then at 5.2, 4.6, and finally at 4.8. Cessation of growth at the lower pH values was not observed. Some of the small crystals grown at pH 4.6 were used as seed crystals in other studies and continued to grow

when placed in a growth environment. The result appears to be a direct effect of pH.

Where microcrystals too small for x-ray diffraction are consistently produced, macromolecule purity is often singled out as the cause. In this respect the strong effect of pH on crystal numbers could be interpreted as the presence of an impurity, where the affinity of the impurity for the lysozyme lattice changes with pH. To avoid heterogeneity possibly introduced by processing steps such as pasteurization and freeze drying (Lorber et al., 1993), the lysozyme used in this study was purified directly from fresh chicken egg white at near-neutral pH. Purity checks with SDS-PAGE using enhanced silver staining and heavy sample overloading have not revealed the presence of any higher molecular mass impurities commonly present in commercial lysozyme preparations. Despite this the presence of impurities cannot be completely dismissed, as impurity proteins may still be present at concentrations below analytical detection limits. In previous lysozyme nucleation studies where impurities were added to make up 1% of the solution concentration, the final number of crystals changed by a factor 2–4 over that of the initial material (Lorber et al., 1993). However, with the highly purified lysozyme used in this study it seems unlikely that impurities below detectable limits (concentrations below 0.01%) would be solely responsible for changes in crystal number by a factor of ~75. Ewing et al. (1996) also indicate that the appearance of bundles of rods or "urchin-like" crystals, as described by Skouri et al. (1995), decrease with increasing purity of the lysozyme solution. Skouri et al. (1995) observed the same trend, in which the proportion of these polycrystalline particles in their purest material was 20–35%. In all of the experimental conditions explored in our study, polycrystals or "urchins" were only observed in some wells at pH 5.2, 18°C, at the lowest initial lysozyme concentration in which crystals grew ($\ln(c/s) = 2.0$). Under these conditions the proportion of polycrystals was only 5%, and the presence of these crystals appear to have had no effect on the tetragonal crystal number or size. Given the trends observed in the previous studies (Skouri et al., 1995; Ewing et al., 1996), this would indicate a high-purity lysozyme preparation.

The change in the crystallization system observed here around pH 4.7 correlates with other unusual observations in the literature. In the work of Cacioppo and Pusey (1991), who have published extensive tetragonal lysozyme phase diagrams, a distinct solubility minimum is observed at pH 4.8 for all temperatures in the range 4–24°C, at 5% (w/v) NaCl. These solubility values were recorded using the same sodium acetate buffer concentration (0.1 M) used in this study. Also in the Roxby and Tanford (1971) titration of denatured lysozyme, a pronounced inflection point is observed in the region of pH 4.7. McPherson (1995) also reports that even in highly purified preparations, where microcrystals are consistently produced, in some instances fine increments in the pH of the crystallization solutions can significantly reduce crystal numbers and increase crystal size. He postulates that this may be due to pH ranges in which basic lysine and arginine side chains or, alternatively, carboxyl aspartic and glutamic acid side chains are titrated. Crystal numbers could then be very precisely controlled by controlling the number of charged groups and their capacity to form intermolecular interactions. This is a more likely explanation for the effect of pH on lysozyme crystal numbers. In terms of nucleation parameters, the titration of side chains that form intermolecular interactions may increase the interfacial tension, thereby decreasing crystal nucleation rates (Mullin, 1993).

For lysozyme there are a number of side-chain groups that have pK values close to or within the pH range 4.0–5.2 (Kuramitsu and Hamaguchi, 1980). Of these groups the C-terminal Leu[129], Asp[48], and His[15] form crystal contacts in tetragonal crystals (Moult et al., 1976). The pK values for these groups measured at 25°C and at 0.1 ionic strength are Leu[129] (3.1), Asp[48] (4.3), and His[15] (5.8) (Kuramitsu and Hamaguchi, 1980). Kuramitsu et al. (1977) report that for lysozyme the pK values of the catalytic groups (Asp[52] and Glu[35]) are independent of temperature. They also report that the pK values increase slightly with ionic strength. If the trends reported in their data are extrapolated to the experimental conditions of this study, an increase in pK values of ~0.1–0.3 pH units above that reported at an ionic strength of 0.1 may be expected. The titration of these groups may modify the interactions between charged groups on opposing molecules, which in turn will affect the ability of these interacting molecules to make successful contacts. It may also effect the strength of the interactions holding molecules together. This would make it more difficult for molecules to interact and form stable nuclei, resulting in a decrease in the nucleation rate. The metastable zone width also increases over this pH range, indicating that a higher driving force is required to generate crystals at the higher pH values.

The decrease in crystal numbers with pH is similar to the result obtained by Ewing et al. (1996), who studied the effect of the solution storage temperature on nucleation rates. In their study a lysozyme solution was split and stored at 37°C and 4°C. By recombining the solutions in set compositions and crystallizing at 20°C, the nucleation rate was found to decrease with increasing content of the 37°C storage material. The decrease in crystal numbers due to storage temperature was thought to be due to a heat-induced conformation change in the molecule, as there is a slight change in lysozyme conformation at temperatures above 20°C (Berthou et al., 1983). Although there is no reported change in tetragonal lysoyzme conformation with pH below 20°C, the two results appear similar in that change in local charge or subtle changes in confirmation seem to have a strong impact on crystal nucleation rates. This is in accordance with lysozyme nucleation work performed by Pusey (1992), in which it was found that increasing solution viscosity by a factor of 50 did not affect nucleation rates, indicating that lysozyme nucleation proceeds slowly relative to the collision rate and is controlled by molecular interaction kinetics.
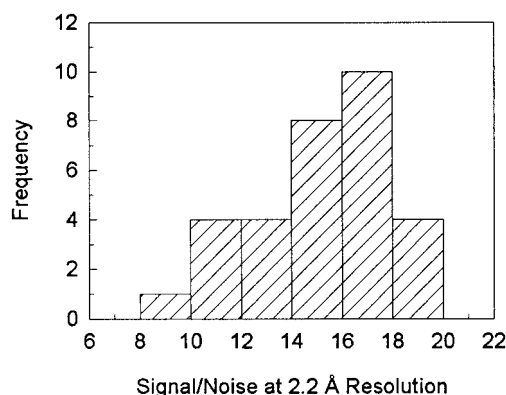
FIGURE 9   Distribution of diffraction characteristics for crystals with unit cell parameter "c" within the range of 38.0–38.1 Å.

Finally, after crystallization conditions have been chosen so as to provide a suitable number of crystals of optimal size and shape, there was still a variation in crystal parameters. Variation in unit cell parameters due to changing relative humidity inside capillaries has previously been reported (Salunke et al., 1985), and part of the variation that we observed (Fig. 7) could have been due to an incomplete sealing or development of microcracks in some of the capillaries. Although a plug of mother liquor was included, water loss would lead to a change in the relative humidity inside the capillary. Trial experiments with water were conducted in both quartz and glass capillaries sealed with epoxy. Water loss did become significant over several days (on the order of 20% in some cases), despite the careful attention paid to the sealing. In light of this, only data within the narrow *c* unit cell region of 38.0–38.1 Å was considered for further analysis. This is the modal region referred to previously, in which the majority of the crystal data fall, and, being a narrow range, the relative humidity is expected to be constant. Even in this smaller sample there is still a striking distribution observed in the diffracting characteristics of the crystals, as illustrated in Fig. 9. For this part of the study a concerted effort was made to prepare the crystallization solutions so that the crystallization plates had the same initial crystallization solution conditions. The average variation from the mean size of up to ±8% indicates, however, that not all of the crystals were likely to have formed in the well at the same time and may have experienced slightly different supersaturation growth environments. This may be part of the reason behind the observed variation in crystal characteristics. One must also be careful in this analysis to point out that a multiplicity of variables are refined in the integration and data reduction process. Errors in any of these only serve to add to the resulting distribution of the x-ray results.

CONCLUSIONS

Although the initial supersaturation and temperature were found to affect the number of lysozyme crystals formed in solution, the largest effect on crystal number and size was that of solution pH. This is thought to be due to changes in charge at localized areas on the molecule's surface, indicating that macromolecule nucleation rates may be very sensitive to changes in molecular charge distribution brought about by changes in solution conditions. Finally, even after crystallization conditions were optimized to produce a suitable number and size of crystals, a variation in crystal parameters was found to exist.

REFERENCES

Alderton, G., and H. L. Fevold. 1946. Direct crystallization of lysozyme from egg white and some crystalline salts of lysozyme. *J. Biol. Chem.* 164:1–5.

Ataka, M., and M. Asai. 1990. Analysis of the nucleation and crystal growth kinetics of lysozyme by a theory of self-assembly. *Biophys. J.* 58:807–811.

Ataka, M., and S. Tanaka. 1986. The growth of large single crystals of lysozyme. *Biopolymers.* 25:337–350.

Aune, K. C., and C. Tanford. 1969. Thermodynamics of the denaturation of lysozyme by guanidine hydrochloride. I. Dependence on pH at 25°C. *Biochemistry.* 8:4579–4585.

Back, J. F. 1984. Changes in the proteins of the vitelline membrane of hens' eggs during storage. *Biochim. Biophys. Acta.* 799:319–321.

Berthou, J., A. Lifchitz, P. Artymiuk, and P. Jolles. 1983. An x-ray study of the physiological-temperature form of hen egg-white lysozyme at 2 Å resolution. *Proc. R. Soc. Lond. Biol.* 217:471–489.

Bessho, Y., M. Ataka, M. Asai, and T. Katsura. 1994. Analysis of the crystallization kinetics of lysozyme using a model with polynuclear growth mechanism. *Biophys. J.* 66:310–313.

Boistelle, R., and J. P. Astier. 1988. Crystallization mechanisms in solution. *J. Crystal Growth.* 90:14–30.

Cacioppo, E., and M. L. Pusey. 1991. The solubility of the tetragonal form of hen egg white lysozyme from pH 4.0 to 5.4. *J. Crystal Growth.* 114:286–292.

Chayen, N. E., J. W. Radcliffe, and D. M. Blow. 1993. Control of nucleation in the crystallization of lysozyme. *Protein Sci.* 2:113–118.

Durbin, S. D., and G. Feher. 1986. Crystal growth studies of lysozyme as a model for protein crystallization. *J. Crystal Growth.* 76:583–592.

Elgersma, A. V., M. Ataka, and T. Katsura. 1992. Kinetic studies on the growth of three crystal forms of lysozyme based on the measurement of protein and Cl⁻ concentration changes. *J. Crystal Growth.* 122:31–40.

Ewing, F. L., E. L. Forsythe, M. Van der Woerd, and M. L. Pusey. 1996. Effects of purification on the crystallization of lysozyme. *J. Crystal Growth.* 160:389–397.

Forsythe, E. L., E. H. Snell, and M. L. Pusey. 1997. Crystallization of chicken egg-white lysozyme from ammonium sulfate. *Acta Crystallogr.* D53:795–797.

Harano, Y., Y. Okamoto, D. L. Asahina, and H. Ooshima. 1989. Nucleation of protein (enzyme thermolysin) from its aqueous solution. *In* Industrial Crystallization '87. J. Nyvlt and S. Zacek, editors. Elsevier, New York. 475–479.

Holmes, K. C., and D. M. Blow. 1966. The Use of X-Ray Diffraction in the Study of Protein and Nucleic Acid Structure. Interscience, New York.

Jolles, P., and J. Berthou. 1972. High temperature crystallization of lysozyme: an example of phase transition. *FEBS Lett.* 23:21–23.

Judge, R. A., E. L. Forsythe, and M. L. Pusey. 1998. The effect of protein impurities on lysozyme crystal growth. *Biotechnol. Bioeng.* 59:776–785.

Judge, R. A., M. R. Johns, and E. T. White. 1995. Protein purification by bulk crystallization: the recovery of ovalbumin. *Biotechnol. Bioeng.* 48:316–323.

Kam, Z., H. B. Shore, and G. Feher. 1978. On the crystallization of proteins. *J. Mol. Biol.* 123:539–555.

King, M. V. 1954. An efficient method for mounting wet protein crystals for x-ray studies. *Acta Crystallogr.* 7:601–605.

Kuramitsu, S., and K. Hamaguchi. 1980. Analysis of the acid-base titration curve of hen lysozyme. *J. Biochem.* 87:1215–1219.

Kuramitsu, S., K. Ikeda, and K. Hamaguchi. 1977. Effects of ionic strength and temperature on the ionization of the catalytic groups, Asp^{52} and Glu^{35}, in hen lysozyme. *J. Biochem.* 82:585–597.

Lorber, B., M. Skouri, J. P. Munch, and R. Giege. 1993. The influence of impurities on protein crystallization: the case of lysozyme. *J. Crystal Growth.* 128:1203–1211.

Malkin, A., and A. McPherson. 1993. Light scattering investigations of protein and virus crystal growth: ferritin, apoferritin and satellite tobacco mosaic virus. *J. Crystal Growth.* 128:1232–1235.

McPherson, A. 1995. Increasing the size of microcrystals by fine sampling of pH limits. *J. Appl. Crystallogr.* 28:362–365.

Mikol, V., E. Hirsch, and R. Giege. 1989. Monitoring protein crystallization by dynamic light scattering. *Fed. Eur. Biochem. Soc. Lett.* 258: 63–66.

Moult, J., A. Yonath, W. Traub, A. Smilansky, A. Podjarny, D. Rabinovich, and A. Saya. 1976. The structure of triclinic lysozyme at 2.5 Å resolution. *J. Mol. Biol.* 100:179–195.

Mullin, J. W. 1993. Crystallization, 3rd Ed. Butterworth-Heinemann, Oxford, England. 176, 194.

Otwinowski, Z., and W. Minor. 1997. Processing of x-ray diffraction data collected in oscillation mode. *Methods Enzymol.* 276A:307–326.

Pusey, M. L. 1991. Estimation of the initial equilibrium constants in the formation of tetragonal lysozyme nuclei. *J. Crystal Growth.* 110:60–65.

Pusey, M. 1992. Continuing adventures in lysozyme crystal growth. *J. Crystal Growth.* 122:1–7.

Rhodes, M. B., P. R. Azari, and R. E. Feeney. 1958. Analysis, fractionation and purification of egg white proteins with cellulose cation exchanger. *J. Biol. Chem.* 230:399–408.

Ries-Kautt, M., and A. Ducruix. 1992. Phase diagrams. *In* Crystallization of Nucleic Acids and Proteins: A Practical Approach. A. Ducruix and R. Giege, editors. Oxford University Press, New York. 195–228.

Roxby, R., and C. Tanford. 1971. Hydrogen ion titration curve of lysozyme in 6 M guanidine hydrochloride. *Biochemistry.* 10:3348–3352.

Salunke, D. M., B. Veerapandian, R. Kodandapani, and M. Vijayan. 1985. Water-mediated transformations in protein crystals. *Acta Crystallogr.* B41:431–436.

Sazaki, G., H. Ooshima, and J. Kato. 1994. Effect of supersaturation ratio on the growth rate and number of protease thermolysin crystals. *J. Crystal Growth.* 135:199–208.

Skouri, M., B. Lorber, R. Giege, J. P. Munch, and J. S. Candau. 1995. Effect of macromolecular impurities on lysozyme solubility and crystallizability: dynamic light scattering, phase diagram, and crystal growth studies. *J. Crystal Growth.* 152:209–220.

Thomas, B. R., P. G. Vekilov, and F. Rosenberger. 1996. Heterogeneity determination and purification of commercial hen egg-white lysozyme. *Acta Crystallogr.* D52:776–784.

Vekilov, P. G., L. A. Monaco, B. R. Thomas, V. Stojanoff, and F. Rosenberger. 1996. Repartitioning of NaCl and protein impurities in lysozyme crystallization. *Acta Crystallogr.* D52:785–798.